Title	Design of a new outer-rotor flux-controllable vernier PM in-wheel motor drive for electric vehicle
Author(s)	Liu, C
Citation	The 2011 International Conference on Electrical Machines and Systems (ICEMS 2011), Beijing, China, 20-23 August 2011. In Proceedings of ICEMS, 2011, p. 1-6
Issued Date	2011
URL	http://hdl.handle.net/10722/160252
Rights	International Conference on Electrical Machines and Systems Proceedings. Copyright © IEEE.

Design of A New Outer-rotor Flux-controllable Vernier PM In-wheel Motor Drive for Electric Vehicle

Chunhua Liu
Department of Electrical and Electronic Engineering, The University of Hong Kong, Hong Kong, China
E-mail: chualiu@eee.hku.hk

Abstract — This paper proposes a new in-wheel motor drive for electric vehicle (EV), which utilizes the outer-rotor topology to directly couple with the tire rims and hence removing the mechanical transmission. The key is to use the vernier structure for obtaining the high-speed to low-speed gear effect and achieving the high output torque at low speed operation. Also, the proposed motor drive adopts the DC field winding for performing the flux weakening control at high speed operation. Thus, this new in-wheel motor drive can smoothly operate within the speed range of 0~1000rpm at different operation modes for EVs. The motor drive and its three-operation modes for EV operation, as well as the steady-state and transient performances are analyzed by using the time-stepping finite-element-method.

I. INTRODUCTION

In recent years, electric vehicles (EVs) are regarded as a friendly candidate for improving environment issue and global warming by greatly reducing the fossil fuels [1]-[11]. Different from the traditional automobiles, the propulsion system of EVs or hybrid EVs (HEVs) utilize the motor drives as the major or auxiliary power facility [12]-[23]. Hence, the propulsion trains of EVs or HEVs have their different topologies from those of the traditional automobiles. In-wheel motor drives, as one of the main propulsion systems for EVs, are very attractive and feasible for practical application, since they have the effective feature of offering the electronic differential action [24]-[28]. Since the speed of the in-wheel motor drive is usually within the range of 0~1000rpm, the motor drive has to be designed either for a low speed gearless type or a high speed gear type [1], [29]-[30]. For the low speed type, it has the advantage of gearless operation, but it has to be designed with the bulky size and heavy weight for achieving the high torque output. For the high speed type, although it removes the drawbacks for heavy weight and large size, it suffers the advantages of acoustic noise transmission loss and regular lubrication.

Vernier PM machines are a new kind of electric machines, which has the attractive merit of offering the high torque output at low speed operation [31]-[36]. Hence, they are proposed to apply for EV application and wind power generation. Also, flux-controllable machines are another new type of electric machines, which are striking for their flexible flux control ability [37]-[39]. Thus, they are also suggested to utilize as the wind generators and EV motors. The purpose of this paper is to artfully integrate these two merits together for proposing a new gearless flux-controllable vernier permanent magnet in-wheel (FCVPM-IW) motor drive for EVs. The key is to use the vernier structure for obtaining the high-speed to low-speed gear effect and hence achieving the high output torque at low speed operation for EVs. Also, this motor drive adopts the DC field winding for performing the flux weakening control at high speed operation. In addition, in order to eliminate the mechanical transmission of in-wheel structures, the outer-rotor topology is adopted for the design of in-wheel motor drive.

Section II will discuss the different configurations of in-wheel motor drives and present the proposed FCVPM-IW type. Section III will be devoted to the proposed machine design, analysis and control. Then, the verification results will be given in Section IV. Finally, Section V will give a conclusion.

II. CONFIGURATION OF IN-WHEEL MOTOR DRIVE

Fig. 1 shows the schematic comparison of different topologies of in-wheel motor drives, including the traditional low-speed gearless type, current high-speed geared type, and proposed FCVPM-IW type. For the traditional low-speed gearless type, it can be seen that the machine with outer-rotor directly coupling with the tire rims. But, it has to be designed with large size for providing the high torque output, which makes the whole structure very bulky and cumbersome. For the current high-speed geared type, it overcomes the bulky motor design by adding a high-to-low speed planetary gear set between the motor rotor and the tire rim. So, the motor can be designed with a normal size for high speed operation. However, the planetary gear set has to be utilized, which increases the complication of the in-wheel drive system and decrease the efficiency of the power transmission. For the proposed FCVPM-IM type, its outer rotor directly connects with the tire rim and hence removing the mechanical transmission. Thus, the proposed in-wheel motor drive achieves the merits of small size and weight, and eliminates the drawbacks due to the mechanical gear.

Fig. 2 gives the schematics of a plug-in EV driving system, which includes the proposed FCVPM-IW motors, the power converter, the controller, and the battery tank. This direct-drive system adopts in-wheel motor drives for four wheels, which can provide the strongly propelling power for EV operation. The in-wheel motors play the role of

electromechanical transmission. And the power converter can adopt the bidirectional type in such a way that the EV energy can be fed back to the battery tank in downhill or braking situation. The controller takes the responsibility of coordinating control of four wheels and the energy management. The battery tank offers the energy storage for charging and discharging. The plug-in inverter is for EV charging with the family 13A plug. Therefore, the proposed in-wheel motor drive system is capable to operate in the following modes, namely the starting or boosting mode, the charging mode, and the steady-speed mode [21], [29].

(*Mode I*.) When the EV begins to launch or needs to accelerate within a short time, the in-wheel motor drive operates in the starting or boosting mode. In this mode, the motor drive should provide the high torque output at the low speed state. Also, the torque can bring the EV entering the normal operation situation.

(*Mode II*.) When the EV goes downhill or runs in braking situation, the in-wheel motor drive works in the charging mode. In this mode, the EV can recover or regenerate the braking energy by the same machine, and hence charging the battery. It means that the in-wheel machine works at the generating mode.

(*Mode III*.) When the EV enters the cruising situation, the in-wheel motor drive runs in the steady-state mode. In this mode, the EV works very smoothly at high speed level and operates in the high efficiency region. Also, it tells that the EV can easily achieve the capability of the continuously variable transmission based on the motor drive control.

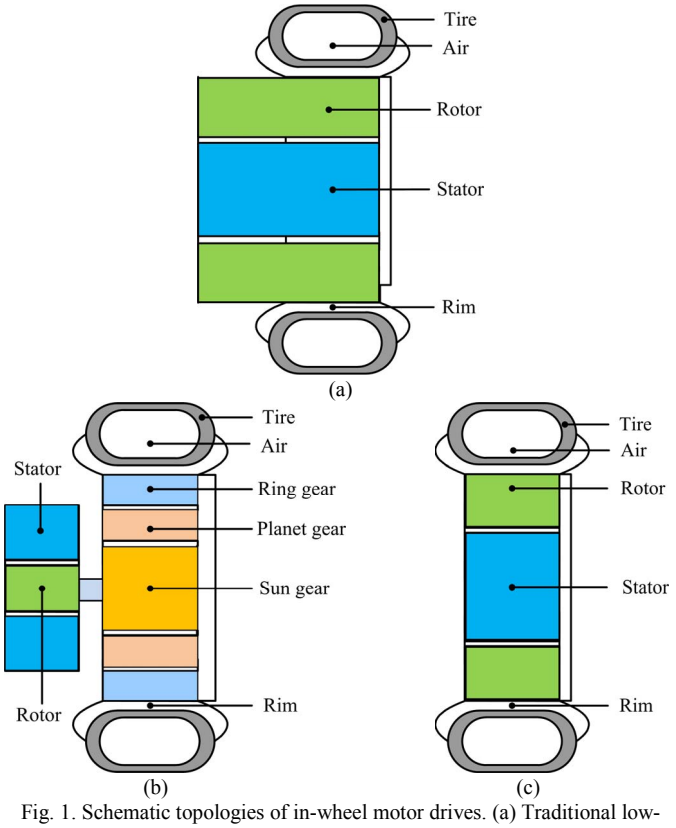

Fig. 1. Schematic topologies of in-wheel motor drives. (a) Traditional low-speed gearless type. (b) Existing high-speed geared type. (c) Proposed FCVPM type.

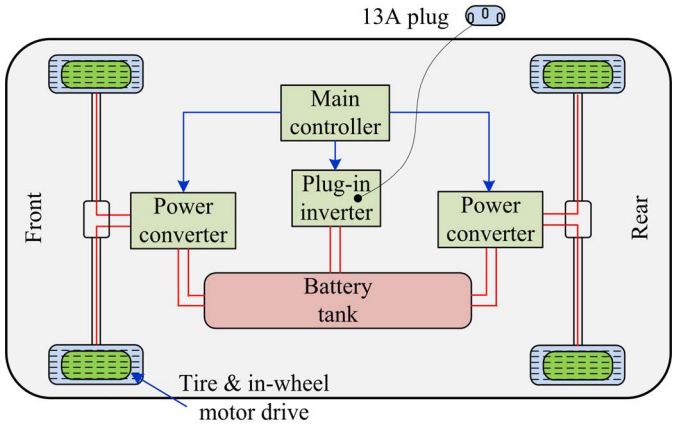

Fig. 2. Schematics of a plug-in EV driving system.

III. Machine Design and Analysis

A. Machine Design

The proposed FCVPM-IM machine structure is shown in Fig. 3, which is an outer-rotor topology [36]. It can be seen that the inner stator accommodates two set of windings, namely the three-phase armature winding and the DC field winding. Also, 24 salient poles are set up in the inner stator for performing the flux modulation and hence obtaining the gear effect. In addition, the outer rotor has 22 pole-pair PMs, which is suitable for intermittent operation and directly coupling with the EV tire rims.

The proposed machine has the vernier structure for its tooth-pole arrangement, which achieves the attractive merit of offering the high torque output at low speed operation. And this merit is very suitable for the starting or boosting mode of the in-wheel motor drive. The basic principle of the tooth-pole arrangement is obeyed the following equations [31]-[33]:

$$N_r = N_s - p_s \tag{1}$$

where N_r is the number of rotor PM pole pairs, N_s is the number of flux-modulation salient poles, and p_s is the number of armature winding pole pairs. Hence, the corresponding high-to-low speed ratio G_r is governed by [31]-[33]:

$$G_r = \frac{\left| ip_s + jN_s \right|}{ip_s} \tag{2}$$

where $i = 1,3,5,\ldots$ and $j = 0,\pm1,\pm2,\ldots$. When $i = 1$ and $j = -1$, the largest space harmonic component is obtained. In addition, the relationship between the N_s and p_s can be given as [36]:

$$N_s = m \times p_s \times k \tag{3}$$

where m is the number of winding phases and k is the flux-modulation poles per phase per armature pole. Usually, it has $k = 2,3,4,5,\ldots$.

Thus, for the proposed in-wheel motor drive, it selects the following parameters of $m = 3$, $p_s = 2$, and $k = 4$. Then, it has $N_s = 24$, $N_r = 22$, and $G_r = 11$, which tells that the rotor speed is only 1/11 of that in stator for armature rotating field speed.

Also, this machine utilizes two set of windings for the armature current control and the field excitation control. Hence, it can obtain the flux weakening ability at high speed operation. And this merit is suitable for the steady-state mode of the in-wheel motor drive. The corresponding principle of the flux control can be referred to the literatures of [37]-[39].

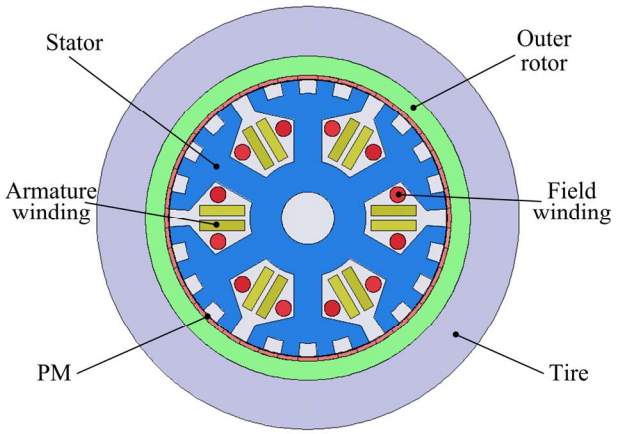

Fig. 1. Magnetization as a function of applied field. Note how the caption is centered in the column.

B. Machine Analysis

The time-stepping finite-element-method (TS-FEM) is utilized for the steady-state and transient performances analysis of the proposed in-wheel motor drive. The mathematic model of the motor drive includes three set of equations, namely the electromagnetic field equations of the machine, the armature circuit equation of the machine, and the motion equation of the motor drive [40]-[44].

$$\Omega: \frac{\partial}{\partial x}\left(v\frac{\partial A}{\partial x}\right)+\frac{\partial}{\partial y}\left(v\frac{\partial A}{\partial y}\right)=-J-v\left(\frac{\partial B_{ry}}{\partial x}-\frac{\partial B_{rx}}{\partial y}\right)+\sigma\frac{\partial A}{\partial t} \quad (4)$$

where Ω is the field solution region, A the magnetic vector potential, J the current density, σ the electrical conductivity, and B_{rx} , B_{ry} the remnant flux density. Second, the armature circuit equation of the machine during motoring is given as

$$u = Ri + L_e\frac{di}{dt}+\frac{l}{S}\iint_{\Omega_e}\frac{\partial A}{\partial t}d\Omega \quad (5)$$

where u is the applied voltage, R the winding resistance, L_e the end winding inductance, l the axial length, S the conductor area of each turn of per phase winding, and Ω_e the total cross-sectional area of conductors of each phase winding. Third, the motion equation of the machine is given by

$$J_m\frac{d\omega}{dt}=T_e-T_L-\lambda\omega \quad (6)$$

where J_m is the moment of inertia, ω the mechanical speed, T_L the load torque, and λ the damping coefficient.

Hence, after the equations of (4) ~ (6) are discretized, the machine model can be deduced and calculated. Consequently, the steady-state and transient performances of the motor drive can be obtained.

C. Control Circuit

Since the proposed in-wheel motor drive has two set of windings (armature winding and DC field winding), the corresponding two set of control circuits of Fig. 4 are used for the two type of current control, namely the armature current control and the DC field current control [12], [15], [21]. For the armature current control, the full-bridge inverter circuit is adopted, which inherently processes the independent phase control and hence achieving the fault-tolerant capability for electrical isolation among phases. Also, this full-bridge circuit can be easily revised as the bidirectional type for the energy feedback to the battery tank. For the field current control, the H-bridge inverter circuit is used, which can readily regulate the amplitude and the direction of the DC current by adjusting the duty cycle of the selected conductive switches.

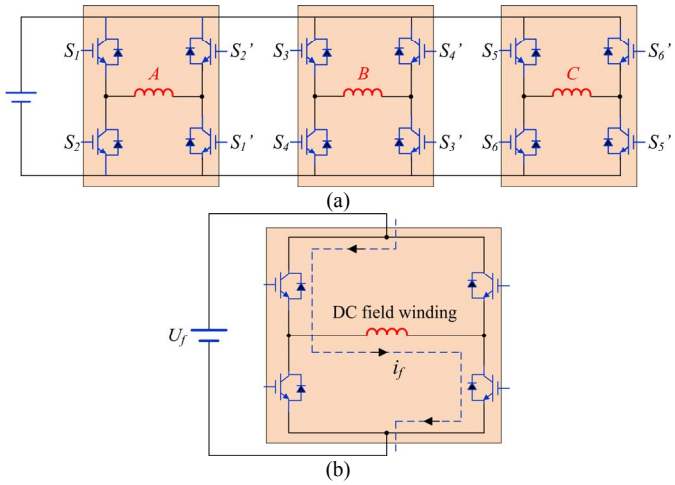

Fig. 4. Control circuits for the proposed in-wheel motor drive. (a) Armature winding control circuit. (b) Field winding control circuit.

IV. Results

The performances of the proposed in-wheel motor drive are calculated and analyzed by the TS-FEM, including the basic characteristics and three operation modes. The corresponding key parameters are given in Table I.

First, the basic characteristics of the proposed in-wheel motor drive are discussed as shown in Fig. 5. From Fig. 5(a) and Fig. 5(b), it can be seen that the airgap flux density has the same pole pairs of the rotor PMs with the value of 22 within 360 degree under the two pole pairs of the stator rotating field. Thus, it verifies that the gear effect and the vernier structure. Also, the average value of the airgap flux density with flux control is obviously less than that of the one without flux control. In addition, from Fig. 5(c), it can be observed that the flux linkage decreases a lot with flux control. Hence, it proves that validity of the flux control for the proposed in-wheel motor drive. Furthermore, Fig. 5(d) shows the cogging torque of the machine, which value is only 3.4% of the steady torque.

Second, the torque performances are given, which can evaluate the capability of the starting or boosting mode of the motor drive. Fig. 6(a) shows the steady-torque of the motor drive under the rated current without flux control. So, it can be derived that with 2 or 3 times of the rated current, this motor

drive can provide the enough propelling power for the EV starting or boosting. In addition, the theoretically operating characteristics of the proposed in-wheel motor drive are given in Fig. 6 (b). It can be observed that the Region I. is for the motor cranking [45]-[50]. The Region II. is for the constant speed operation where the motor drive can be further boosted for a higher torque output, such as the hill climbing.

Third, the charging mode of this motor drive is evaluated. Fig. 7(a) shows the no-load EMF of the machine, which operates at 600rpm. It tells that during the downhill operation or braking situation, the machine can feed back the energy to the battery tank. The corresponding theoretically rectified voltage is about 767V after the capacitor filtering, which is given in Fig. 7(b). Hence, it can be further regulated to the suitable battery charging voltage by the DC-DC converter.

Forth, the flux weakening ability of the proposed motor drive is studied, which can evaluate the smooth operation for the steady-state of the motor drive. Fig. 8(a) shows the flux linkage waveforms under 1000rpm with different field currents. It can be observed that with different field current, the flux linkages can be readily tuned down, hence proving the tuning ability of the proposed motor drive, as well as obtaining the desired electromagnetic parameters. Furthermore, Fig. 8(b) gives the theoretically torque capability under different EV operating speeds. It can be seen that with flux weakening control, the motor drive can work in the constant power region, and hence improving the performance of EV operation.

TABLE I
PARAMETERS OF IN-WHEEL MOTOR DRIVE

Item	Value
Armature winding	3 phases AC current
Field winding	DC current
Speed range	0~1000 rpm
Rated torque	90 Nm
Number of rotor PM pole pairs	22
Number of flux modulation poles	24
Number of field winding poles	6
Number of armature winding pole pairs	2
Number of flux modulation poles per phase per armature pole	4
Diameter of rotor outside	246.0 mm
Diameter of rotor inside	211.2 mm
Diameter of stator outside	210.0 mm
Diameter of shaft	40.0 mm
Stack length	80.0 mm
Airgap length	0.6 mm
Yoke material	Iron steel
PM material	Nd-Fe-B

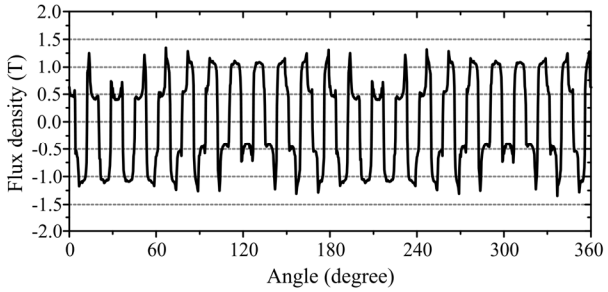

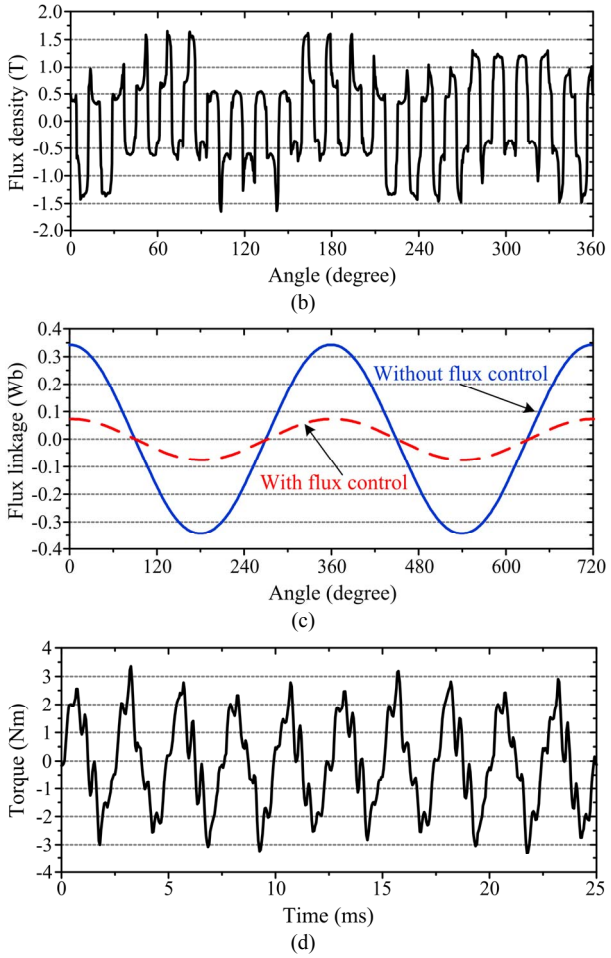

Fig. 5. Basic characteristics of proposed in-wheel motor drive. (a) Airgap flux density without flux control. (b) Airgap flux density with flux control. (c) Flux linkages. (d) Cogging torque.

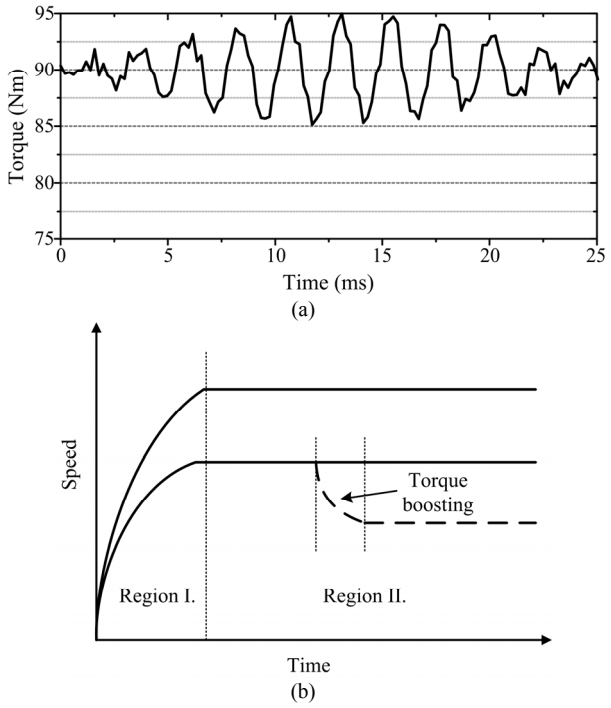

Fig. 6. Mode I: Starting or booting performances. (a) Steady torque under rated currents. (b) Theoretically operating characteristics.

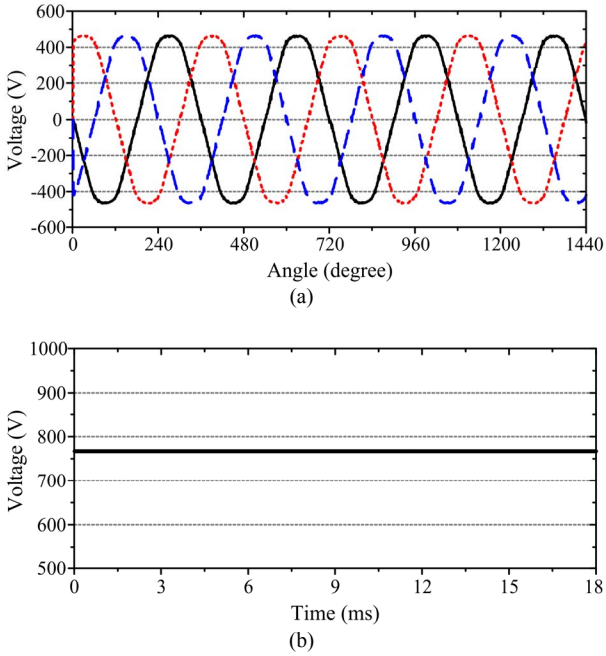

Fig. 7. Mode II: Charging performances. (a) No-load EMF waveform. (b) Theoretically rectified voltage.

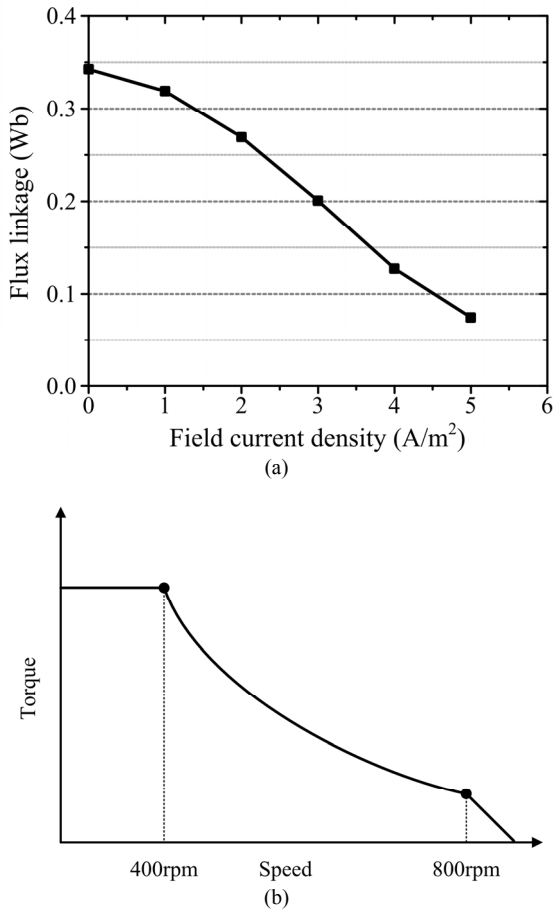

Fig. 8. Mode III: Flux weakening ability. (a) Flux linkage amplitudes with different field currents. (b) Theoretically torque capability.

V. Conclusion

In this paper, a new direct-drive in-wheel motor drive is proposed, which adopts the vernier structure and double winding concept for performing the gear effect and flux control. The inherent outer-rotor topology make the machine easily connect with the wheel rim and removes the drawback of the mechanical transmission. Also, its vernier structure benefits the high torque output at low speed operation. Additionally, the created DC field winding helps the motor drive readily obtaining the flux weakening control at high speed operation. TS-FEM model is built up and verifies the validity of the motor drive design. Also, three-operation modes of the in-wheel motor drive are studied, which shows the feasibility of the motor drive applying for EVs.

Acknowledgment

This work was supported and funded by the grants of HKU Small Project Funding 201007176302, The University of Hong Kong, Hong Kong Special Administrator Region, China

References

[1] C.C. Chan and K.T. Chau, *Modern Electric Vehicle Technology*. Oxford University Press, November 2001, 352 pages.

[2] C.C. Chan, "The state of the art of electric, hybrid and fuel cell vehicles," Proceeding of IEEE, vol. 95, no. 4, April 2007, pp. 704-718.

[3] M. Ehsani, Y. Gao, and J.M. Miller, "Hybrid electric vehicles: architecture and motor drives," Proceeding of IEEE, vol. 95, no. 4, April 2007, pp. 719-728.

[4] C.C. Chan and K.T. Chau, "An overview of power electronics in electric vehicles," IEEE Transactions on Industrial Electronics, vol. 44, no. 1, February 1997, pp. 3-13.

[5] D.W. Gao, C. Mi, and A. Emadi, "Modeling and simulation of electric and hybrid vehicles," Proceeding of IEEE, vol. 95, no. 4, April 2007, pp. 729-745.

[6] K.T. Chau and C.C. Chan, "Electric vehicle technology - a timely course for electrical engineering students," International Journal of Electrical Engineering Education, vol. 35, no. 3, July 1998, pp. 212-220.

[7] K. Okura, "Development and future issues of high voltage systems for FCV," Proceeding of IEEE, vol. 95, no. 4, April 2007, pp. 790-795.

[8] K.T. Chau, Y.S. Wong and C.C. Chan, "An overview of energy sources for electric vehicles," Energy Conversion and Management, vol. 40, no. 10, July 1999, pp. 1021-1039.

[9] K.T. Chau, K.C. Wu, C.C. Chan and W.X. Shen, "A new battery capacity indicator for nickel-metal hydride battery powered electric vehicles using adaptive neuro-fuzzy inference system," Energy Conversion and Management, vol. 44, no. 13, August 2003, pp. 2059-2071.

[10] K.T. Chau and Z. Wang, "Overview of power electronic drives for electric vehicles," HAIT Journal of Science and Engineering - B: Applied Sciences and Engineering, vol. 2, no. 5-6, December 2005, pp. 737-761.

[11] K.T. Chau and C.C. Chan, "Emerging energy-efficient technologies for hybrid electric vehicles," Proceedings of IEEE, vol. 95, no. 4, April 2007, pp. 821-835.

[12] K.T. Chau, C.C. Chau, and C. Liu, "Overview of permanent magnet brushless drives for electric and hybrid electric vehicles," IEEE Transactions on Industrial Electronics, Vol. 55, No. 6, pp. 2246-2257, June 2008.

[13] C. Liu, K.T. Chau, J.Z. Jiang, and S. Niu, "Comparison of stator-permanent-magnet brushless machines," IEEE Transactions on Magnetics, Vol. 44, No. 11, pp. 4405-4408, Nov. 2008.

[14] X. Zhu, M. Cheng, K.T. Chau and C. Yu, "Torque ripple minimization of flux-controllable stator-permanent-magnet brushless motors using harmonic current injection," Journal of Applied Physics, vol. 105, no. 7, April 2009, paper no. 07F102, pp. 1-3.

[15] Z.Q. Zhu and D. Howe, "Electrical machines and drives for electric, hybrid and fuel cell vehicles," Proceedings of IEEE, vol. 95, no. 4, April 2007, pp. 746-765.

[16] C. Liu, K.T. Chau, W. Li, and C. Yu, "Efficiency optimization of a permanent-magnet hybrid brushless machine using DC field current control," IEEE Transactions on Magnetics, Vol. 45, No. 10, pp. 4652-4655, October 2009.
[17] W. Zhao, K.T. Chau, M. Cheng, J. Ji and X. Zhu, "Remedial brushless AC operation of fault-tolerant doubly-salient permanent-magnet motor drives," IEEE Transactions on Industrial Electronics, vol. 57, no. 6, June 2010, pp. 2134-2141.
[18] C. Liu, K.T. Chau, and W. Li, "Comparison of fault-tolerant operations for permanent-magnet hybrid brushless motor drive," IEEE Transactions on Magnetics, Vol. 46, No. 6, pp. 1378-1381, June 2010.
[19] Y. Fan and K.T. Chau, "Design, modeling, and analysis of a brushless doubly fed doubly salient machine for electric vehicles," IEEE Transactions on Industry Applications, vol. 44, no. 3, May-June 2008, pp. 727-734.
[20] C. Liu, K.T. Chau, and W. Li, "Loss analysis of permanent magnet hybrid brushless machines with and without HTS field windings," IEEE Transactions on Applied Superconductivity, Vol. 20, No. 3, pp. 1077-1080, June 2010.
[21] C. Liu, K.T. Chau, and J.Z. Jiang, "A permanent-magnet hybrid brushless integrated- starter-generator for hybrid electric vehicles," IEEE Transactions on Industrial Electronics, Vol. 57, No. 12, pp. 4055-4064, December 2010.
[22] C. Liu, K.T. Chau, and W. Li, "Design and Analysis of a HTS Brushless Doubly-fed Doubly-salient Machine," IEEE Transactions on Applied Superconductivity, vol 21, no.3, pp. 1119-1122 June 2011.
[23] M. Cheng, K.T. Chau, C.C. Chan and Q. Sun, "Control and operation of a new 8/6-pole doubly salient permanent magnet motor drive," IEEE Transactions on Industry Applications, vol. 39, no. 5, September/October 2003, pp. 1363-1371.
[24] C. Feng, X. Jing, G. Bin, C. Shukang, and Z. Jiange, "Double-stator permanent magnet synchronous in-wheel motor for hybrid electric drive system," IEEE Transactions on Industrial Electronics, Vol. 45, No. 1, pp. 278-281, Jan. 2009.
[25] K.T. Chau, D. Zhang, J.Z. Jiang, C. Liu and Y.J. Zhang, "Design of a magnetic-geared outer-rotor permanent-magnet brushless motor for electric vehicles," IEEE Transactions on Magnetics, vol. 43, no. 6, June 2007, pp. 2504-2506.
[26] Y. Hori, "Future vehicle driven by electricity and control - research on four-wheel-motored 'UOT Electric March II' ," IEEE Transactions on Industrial Electronics, Vol. 51, No. 5, pp. 954-962, Oct. 2004.
[27] T.F. Chan, L.-T. Yan, and S.-Y. Fang, "In-wheel permanent-magnet brushless dc motor drive for an electric bicycle," IEEE Transactions on Energy Conversion, vol. 17, no. 2, pp. 229-233, June 2002.
[28] M. Terashima, T. Ashikaga, T. Mizuno, K. Natori, N. Fujiwara, and M. Yada, "Novel motors and controllers for high-performance electriv vehicle with four in-wheel motors," IEEE Transactions on Industrial Electronics, vol. 44, no. 1, pp. 28-38, Feb. 1997.
[29] K.T. Chau, C. Liu, and J.Z. Jiang "Comparison of outer-rotor stator-permanent-magnet brushless motor drives for electric vehicles," Proceedings of International Conference of Electrical Machines and Systems (ICEMS2008), Wuhan, China, Oct. 2008, Paper No. 699793, pp. 2842-2847.
[30] S.-I. Sakai, H. Sado, and Y. Hori, "Motor control in an electric vehicle with four independently driven in-wheel motors," IEEE/ASME Transactions on Mechatronics, vol. 4, no. 1, pp. 9-16, March 1999.
[31] A. Toba and T.A. Lipo, "Novel dual-excitation permanent magnet vernier machine," IEEE Industry Applications Conference (IAS1999), 34th IAS Annual Meeting, vol. 4, 1999, pp. 2539-2544.
[32] A. Toba and T.A. Lipo, "Generic torque-maximizing design methodology of surface permanent-magnet vernier machine," IEEE Transactions on Industry Applications, vol. 36, no. 6, Nov. 2000, pp. 1539-1546.
[33] J. Li, K.T. Chau, J.Z. Jiang, C. Liu and W. Li, "A new efficient permanent-magnet vernier machine for wind power generation," IEEE Transactions on Magnetics, vol. 45, no. 6, June 2010, pp. 1475-1478.
[34] S. Niu, S.L. Ho, W.N. Fu, and L.L. Wang, "Quantitative comparison of novel vernier permanent magnet machines," IEEE Transactions on Magnetics, vol. 46, no. 6, June 2010, pp. 2032-2035.
[35] S. Niu, S.L. Ho, and W.N. Fu, "A novel direct-drive dual-structure permanent magnet machine," IEEE Transactions on Magnetics, vol. 46, no. 6, June 2010, pp. 2036-2039
[36] C. Liu, J. Zhong, and K.T. Chau, "A novel flux-controllable vernier permanent-magnet machine," accepted for publication in IEEE Transactions on Magnetics, 2011.
[37] C. Liu, K.T. Chau, and J.Z. Jiang, "Design of a new outer-rotor permanent-magnet hybrid machine for wind power generation," IEEE Transactions on Magnetics, Vol. 44, No. 6, pp. 1494-1497, June 2008.
[38] J.A. Tapia, F. Leonardi, and T.A. Lipo, "Consequent-pole permanent-magnet machine with extended field-weakening capabili5y," IEEE Transactions on Industry Applications, vol. 39, no. 6, Nov./Dec. 2003, pp. 1704-1709.
[39] C. Liu, K.T. Chau, and X. Zhang, "An efficient wind-photovoltaic hybrid generation system using doubly-excited permanent-magnet brushless machine," IEEE Transactions on Industrial Electronics, Vol. 57, No. 3, pp. 831-839, March 2010.
[40] Y. Wang, K.T. Chau, C.C. Chan, and J.Z. Jiang, "Transient analysis of a new outer-rotor permanent-magnet brushless dc drive using circuit-field-torque time-stepping finite element method," IEEE Transactions on Magnetics, vol. 38, no. 2, March 2002, pp. 1297-1300.
[41] S.J. Salon, *Finite element Analysis of electrical Machines*, Kluwer Academic Publisher, Boston USA, 1995.
[42] L. Jian and K.T. Chau, "Analytical calculation of magnetic field distribution in coaxial magnetic gears," Progress In Electromagnetics Research, vol. 92, 2009, pp. 1-16.
[43] T. Lubin, t. Hamiti, H. razik, and A. Rezzou, "Comparison between finite-element analysis and winding function theory for inductances and torque calculation of a synchronous reluctance machine," IEEE Transactions on Magnetics, vol. 43, no. 8, August 2007, pp. 4704-4707.
[44] Y. Gong, K.T. Chau, J.Z. Jiang, C. Yu and W. Li, "Design of doubly salient permanent magnet motors with minimum torque ripple," IEEE Transactions on Magnetics, vol. 45, no. 10, October 2009, pp. 4704-4707.
[45] T.M. Johns, "Motion control with permanent magnet AC machines," Proceedings of IEEE, Vol. 82, No. 8, pp. 1241-1252, August 1994
[46] Y. Liao and T.A. Lipo, "A new doubly salient permanent magnet motor for adjustable speed drives," Electric Machines and Power Systems, Vol. 22, No. 1, pp. 259-270, 1994.
[47] T.J.E. Miller, Brushless Permanent Magnet and Reluctance Motor Drives, Clarendon Press, Oxford, 1989.
[48] P.C. Sen, "Electric motor drives and control-past, present and future," IEEE Transactions on Industrial Electronics, Vol. 37, No. 6, pp. 562-575, Dec., 1990.
[49] J.A. Tapia, F. Leonardi, and T.A. Lipo, "Consequent-pole permanent-magnet machine with extended field-weakening capability," IEEE Transaction on Industry Applications, Vol. 39, No. 6, pp. 1704-1709, Nov./Dec. 2003.
[50] S.Z. Jiang, K.T. Chau and C.C. Chan, "Spectral analysis of a new six-phase pole-changing induction motor drive for electric vehicles," IEEE Transactions on Industrial Electronics, Vol. 50, No. 1, pp. 123-131, February 2003.